HHS Public Access

Author manuscript

J Biomech. Author manuscript; available in PMC 2021 September 18.

Published in final edited form as:

J Biomech. 2020 September 18; 110: 109968. doi:10.1016/j.jbiomech.2020.109968.

Dysplastic hip anatomy alters muscle moment arm lengths, lines of action, and contributions to joint reaction forces during gait

Ke Song[a,b], **Brecca M.M. Gaffney**[a], **Kevin B. Shelburne**[c], **Cecilia Pascual-Garrido**[d], **John C. Clohisy**[d], **Michael D. Harris**[a,b,d,*]

[a]Program in Physical Therapy, Washington University in St. Louis School of Medicine, St. Louis, MO, USA

[b]Department of Mechanical Engineering and Materials Science, Washington University in St. Louis, St. Louis, MO, USA

[c]Department of Mechanical and Materials Engineering, University of Denver, Denver, CO, USA

[d]Department of Orthopaedic Surgery, Washington University in St. Louis School of Medicine, St. Louis, MO, USA

Abstract

Developmental dysplasia of the hip (DDH) is characterized by abnormal bony anatomy, which causes detrimental hip joint loading and leads to secondary osteoarthritis. Hip joint loading depends, in part, on muscle-induced joint reaction forces (JRFs), and therefore, is influenced by hip muscle moment arm lengths (MALs) and lines of action (LoAs). The current study used subject-specific musculoskeletal models and in-vivo motion analysis to quantify the effects of DDH bony anatomy on dynamic muscle MALs, LoAs, and their contributions to JRF peaks during early (~17%) and late-stance (~52%) of gait. Compared to healthy hips (N = 15, 16–39 y/o), the abductor muscles in patients with untreated DDH (N = 15, 16–39 y/o) had smaller abduction MALs (e.g. anterior gluteus medius, 35.3 vs. 41.6 mm in early stance, 45.4 vs. 52.6 mm late stance, $p \leq 0.01$) and more medially-directed LoAs. Abduction-adduction and rotation MALs also differed for major hip flexors such as rectus femoris and iliacus. The altered MALs in DDH corresponded to higher hip abductor forces, medial JRFs (1.26 vs. 0.87 × BW early stance, $p = 0.03$), and resultant JRFs (5.71 vs. 4.97 × BW late stance, $p = 0.05$). DDH anatomy not only affected hip muscle force generation in the primary plane of function, but also their out-of-plane mechanics, which collectively elevated JRFs. Overall, hip muscle MALs and their contributions to JRFs were significantly altered by DDH bony anatomy. Therefore, to better understand the mechanisms of joint degeneration and improve the efficacy of treatments for DDH, the dynamic anatomy-force relationships and multi-planar functions of the whole hip musculature must be collectively considered.

*Corresponding author at: 4444 Forest Park Avenue, Suite 1101, Campus Box 8502, St. Louis, MO 63108-2212, USA. harrismi@wustl.edu (M.D. Harris).

Declaration of Competing Interest

The authors declare that they have no known competing financial interests or personal relationships that could have appeared to influence the work reported in this paper.

Appendix A. Supplementary material

Supplementary data to this article can be found online at https://doi.org/10.1016/j.jbiomech.2020.109968.

Keywords

Developmental dysplasia of the hip; Muscle moment arm; Line of action; Joint reaction force; Musculoskeletal modeling

1. Introduction

Developmental dysplasia of the hip (DDH) is characterized by abnormal acetabular and femoral anatomy (Wyles et al., 2017). When untreated, these abnormalities alter hip intra-articular loading, cause tissue damage, and increase the risk of early secondary osteoarthritis (Groh and Herrera, 2009; Lewis and Sahrmann, 2006). Muscle forces and joint reaction forces (JRFs) are major mechanical contributors to hip joint loading (Correa et al., 2010), and are found to be altered in patients with untreated DDH (Skalshoi et al., 2015; Harris et al., 2017). It has been speculated that the abnormal bony features of DDH, such as lateralized hip joint centers (HJCs), are the sources of altered muscle-induced loading (Cheng et al., 2019; Maquet, 1999), but the relationships that explain how bony anatomy alters muscle and joint forces have not been explicitly established.

Among factors influencing muscle mechanics, the ability of muscles to generate forces and moments around a joint is directly affected by their anatomical paths. Two key mechanical parameters that describe the anatomy-force relationships of muscles are their moment arm lengths (MALs) and lines of action (LoA). MALs, defined as the perpendicular distance from the joint center to the muscle LoA, represent the effectiveness of muscles at generating moments to rotate the joint (Pandy, 1999; Sherman et al., 2013). If a muscle MAL is reduced, higher force from that muscle is needed to generate the same joint moment. LoAs dictate the direction of muscle forces, which affects muscle contributions to loading within the joint (Yanagawa et al., 2008). The MALs and LoAs of multiple muscles collectively influence compressive and shear forces borne by the joint (Yanagawa et al., 2008). A few radiographic reports and theoretical models have suggested that abnormal bony anatomy in untreated DDH reduces hip abductor MALs and alters their medio-lateral LoAs in a way that may increase hip articular pressure (Liu et al., 2012; Maquet, 1999). These studies provided preliminary insight into the links between DDH bony anatomy and muscle-induced joint loading, but were limited to the abductor muscles in a static position. Because muscle paths vary with joint positions, their dynamic force-generating abilities induce variable joint loading during an activity, and therefore lead to motion-specific risks for tissue damage. However, no study has reported MALs and LoAs in patients with untreated DDH during dynamic motions, and how they collectively contribute to hip JRFs.

Because muscle forces cannot be measured directly during motion, musculoskeletal models have been used to quantify dynamic hip muscle MALs and LoAs (Delp et al., 1999; Arnold et al., 2000; Blemker and Delp, 2005) and their contributions to JRFs (Scheys et al., 2008; van Arkel et al., 2013; Wesseling et al., 2016b). The default generic geometry in most musculoskeletal models represents healthy bony anatomy, which makes such models less reliable for estimating muscle mechanics in populations with anatomical deformities (Scheys et al., 2008). Therefore, including subject-specific anatomy is important for

estimating hip mechanics in DDH (Song et al., 2019), and has helped elucidate significant hip JRF differences compared to healthy controls (Harris et al., 2017). However, these recent models of DDH fell short of establishing the underlying relationships between the muscle-induced hip joint loading (e.g. JRFs) of DDH and the bony deformity. As such, the potentially vital roles of muscle anatomy-force parameters (MALs, LoAs) in the patho-mechanics of DDH also remain unclear.

The objective of this study was to quantify how hip muscle MALs, LoAs, and their contributions to hip JRFs during gait are altered in patients with untreated DDH compared to healthy controls. We hypothesized that patients with DDH would have smaller hip abductor MALs and more medially-directed LoAs due to lateralized HJCs (Cheng et al., 2019), which would result in higher medially-directed hip muscle forces and JRFs (Harris et al., 2017).

2. Methods

2.1. Subjects and data collection

With Institutional Review Board approval and informed consent, 15 female patients with untreated DDH (age: 16–39 y/o) and 15 female healthy controls (age: 16–39 y/o) were included (Table 1). An *a priori* power analysis (Faul et al., 2007) based on prior hip JRF findings (Harris et al, 2017) indicated 15 subjects per group could detect inter-group differences with power of 0.8. Patients were diagnosed by a single orthopaedic surgeon (JCC), had hip pain lasting at least 3 months, and radiographic evidence of DDH determined by a lateral center edge angle <20° (Wiberg, 1939). For each DDH patient, the symptomatic hip was chosen for analysis. Healthy controls had no self-reported history of hip pathology, and no pain or discomfort during a flexion-adduction-internal-rotation clinical screening exam (MacDonald et al., 1997). A random side was chosen for comparison with DDH patients. Both groups had no previous hip surgeries, other lower extremity diseases, or pain that limited functional activities. Magnetic resonance (MR) images were collected from the psoas major muscle origin to the knees using a 3T scanner (VIDA, Siemens AG; Munich, Germany) with T1-weighted VIBE gradient-echo sequences and SPAIR fat suppression (1 × 1 × 1 mm voxels). During imaging, subjects were prone with the hip positioned at approximately zero degrees flexion, adduction, and rotation. From the MR images, 3D geometries of the pelvis and femurs for each subject were reconstructed using Amira software (Thermo Fisher Scientific, Houston, TX).

Full-body gait data were collected using 70 retro-reflective markers while subjects walked at a self-selected speed on an instrumented treadmill (Bertec; Columbus, OH), with a 5-minute warm-up (Zeni and Higginson, 2010). Marker trajectories were collected at 100 Hz using 10 infrared cameras (Vicon; Centennial, CO). Ground reaction forces were collected at 2000 Hz by the treadmill. Fourth-order Butterworth low-pass filters were applied to marker data using an 8 Hz cutoff determined with residual analysis (Winter, 2004), and a 6 Hz cutoff for force data to reduce analog noise on instrumented treadmills (Pickle et al., 2016).

2.2. Musculoskeletal modeling

Subject-specific musculoskeletal models were created from an existing OpenSim model (Lai et al., 2017), similar to procedures recently described (Song et al., 2019). The generic model was modified by adding torso and hip external rotator muscles (Table 2) with experimental-based paths and strengths (Shelburne et al., 2010; Handsfield et al., 2014), yielding 98 muscle–tendon actuators. Then, MR-based 3D pelvis and femur geometries were substituted into the model for each subject (Fig. 1A). HJCs were moved to subject-specific locations, determined as the centroid of a sphere fit to the 3D-reconstructed femoral head (Harris et al., 2017). Each MR femur was then rotated about the subject-specific HJC until the femoral shaft axis and the distal trans-epicondyle axis were both aligned to the generic geometries.

Origin and insertion sites of the hip muscles were then updated on the subject-specific pelvis and femurs based on reconstructed bone-muscle geometries, MR images, and anatomical guidelines (Netter, 2014) (Fig. 1A). Via points approximating nonlinear muscle paths (e.g. tensor fasciae latae) and wrapping objects for the iliacus and psoas major muscles were also updated, using the MR images as a guide (Wesseling et al., 2016a). The remaining model segments were non-uniformly scaled in antero-posterior (AP), supero-inferior (SI), and medio-lateral (ML) dimensions using experimental marker data. Muscle optimal fiber lengths and tendon slack lengths were linearly scaled from the generic model according to the total length of updated muscle paths in each subject-specific model (Wesseling et al., 2016a), which assumed no muscle architecture adaptations (e.g. sarcomere loss) had occurred due to the DDH anatomy.

Hip and pelvis angles were calculated via inverse kinematics, and internal hip moments were calculated via inverse dynamics (Winter, 2004), for each subject across a representative gait cycle. Residual reduction was applied to minimize the nonphysical residual forces and moments and maintain dynamic consistency within inverse dynamics results (Delp et al., 2007). Muscle forces were estimated using static optimization that minimized the sum-square of muscle activations (Anderson and Pandy, 2001). The forces of individual hip muscles were then summed by functional groups (Lai et al., 2017; Shelburne et al., 2010; Table 2). Lastly, resultant hip JRFs and AP, SI, ML directional components were calculated from muscle forces (Steele et al., 2012) and expressed in the pelvis frame to represent loading on the acetabulum.

Subject-specific MALs and LoAs for all hip muscles were extracted across the entire gait cycle. Dynamic muscle MALs (Fig. 1B) were computed within OpenSim using a generalized force approach (Sherman et al., 2013). Hip muscle LoAs were extracted using an established method (van Arkel et al., 2013) and expressed as unit vectors with AP, SI, and ML components in the pelvis frame (Fig. 1C). Individual muscle forces were decomposed along each LoA component to determine the proportion of that muscle's net force in the AP, SI, ML directions. These three muscle force components were also each summed by functional groups.

2.3. Model validation

The subject-specific models were validated using established methods (Hicks et al., 2015). First, model-estimated muscle activations were compared to surface electromyography (EMG) signals. EMG during gait was collected from bilateral gluteus maximus, gluteus medius, rectus femoris, tensor fasciae latae, biceps femoris long head, vastus lateralis, medial gastrocnemius, and erector spinae, following SENIAM guidelines (Hermens et al., 2000). Signals were recorded at 2000 Hz using a 16-channel system (MA300-XVI, Motion Lab Systems Inc.; Baton Rouge, LA), shifted by 1.2 ms to offset wireless latency, band-pass filtered with 10–350 Hz cutoffs, rectified, and smoothed with a 10 Hz fourth-order Butterworth low-pass filter (De Luca et al., 2010). Model-estimated muscle activations from static optimization were reported on a scale of 0 (none) to 1 (maximum). For comparison, EMG signals in each trial were also normalized to a 0-to-1 scale relative to the maximum within that trial (Steele et al., 2012). Second, model errors and residuals were ensured to be within limits recommended for gait simulations (Hicks et al., 2015), for both motion tracking (root-mean-square marker error <2 cm) and static optimization (residual force <5% × BW, moment <0.5 Nm/kg). Finally, estimated hip JRFs and muscle forces were qualitatively compared to recent subject-specific modeling studies to ensure they are within 2 standard deviations of previously reported values (Hicks et al., 2015, Wesseling et al., 2016a, Wesseling et al., 2016b, Harris et al., 2017, Song et al., 2019).

2.4. Data analysis

Hip muscle LoAs, MALs, individual and grouped muscle forces, hip JRFs, as well as joint angles and moments were time-normalized to the gait cycle. JRFs and muscle forces were normalized by body weight (× BW), while joint moments were normalized by body mass (Nm/kg) (Moisio et al., 2003). Peak resultant hip JRFs in early stance (~17% of gait cycle, termed ‘JRF1′) and late stance (~52% of gait cycle, termed ‘JRF2′) were determined, as well as joint angles and moments at these two time points. LoAs, MALs and forces for all muscles crossing the analyzed hip (Table 2) were extracted at JRF1 and JRF2. Within each functional group, the muscles that produced the maximum force at JRF1 or JRF2 were categorized as the primary dependent variables for statistical comparisons. The other individual muscles were categorized as secondary variables.

All variables were examined with the Shapiro-Wilk test for normality and Levene’s test for homogeneity of variance. Normally distributed variables were compared between Healthy and DDH groups using independent t-tests, with corrections for unequal variances. Other variables were compared non-parametrically using Mann-Whitney U tests. Statistical significance for each test was $\alpha = 0.05$. Effect sizes for inter-group differences were determined with Cohen’s d (Cohen, 1988) and classified as small ($0.2 \leq d < 0.5$), medium ($0.5 \leq d < 0.8$), or large ($d \geq 0.8$). Primary variables compared between DDH and Healthy were LoAs, MALs, and forces of muscles selected from each functional group, and hip JRFs. Secondary variables were LoAs, MALs, and forces of other individual muscles, as well as joint angles and moments. To further quantify the bony features of untreated DDH that may directly influence muscle anatomy-force relationships, especially the relative lateralization of HJCs (Cheng et al., 2019), the ML location of HJC was normalized by the ML distance between the anterior superior iliac spine and the mid-sagittal plane, then

compared between groups. The depth, height, and width of the pelvises were also compared between the DDH and Healthy subjects.

3. Results

3.1. Subject characteristics and model validation

There were no significant differences between DDH and Healthy groups in age, height, mass, body-mass index, walking speed (Table 1), and pelvis dimensions. Compared to Healthy subjects, HJCs were significantly lateralized in DDH. Model-estimated muscle activation qualitatively agreed with EMG timings (Suppl. Fig. 1). Model motion tracking errors, residual forces and moments were under 2 cm, 0.025 × BW and 0.4 Nm/kg, respectively (Suppl. Fig. 2). Hip muscle forces and JRFs were in ranges similar to recent subject-specific modeling studies.

3.2. Hip muscle MALs and LoAs

Compared to Healthy, DDH subjects had significantly different hip abduction–adduction and rotation MALs (Table 3, Fig. 2). Specifically, abduction MALs were smaller for the primary hip abductors (e.g. gluteus medius, $p \leq 0.03$, $d \geq 0.83$), and flipped from abduction to adduction roles for the flexors (e.g. iliacus, $p < 0.01$, $d \geq 1.30$) throughout stance. Additionally, internal rotation MALs of the iliacus were significantly smaller in DDH ($p \leq 0.02$, $d \geq 0.93$). Hip flexion–extension MALs were not different between groups for any muscle.

For DDH subjects, muscle LoAs significantly differed for the gluteus maximus, which was directed more medially compared to Healthy ($p = 0.02$, $d = 0.92$ at JRF1; Table 3, Fig. 2). No other LoAs were significantly different between DDH and Healthy groups, although the anterior section of gluteus medius also trended towards a more medial orientation in DDH at JRF1 ($p = 0.06$, $d = 0.71$; Suppl. Table 2).

3.3. Hip muscle forces and JRFs

Resultant muscle forces differed between DDH and Healthy for the hip abductors and internal rotators. Abductor forces were significantly higher in the DDH group throughout stance ($p \leq 0.02$, $d \geq 0.88$; Fig. 3). Internal rotator forces were also higher in DDH ($p \leq 0.04$, $d \geq 0.78$), as many concurrently served abductor roles (Table 2). Muscle force components were also higher in the DDH group for both abductors and internal rotators in the superior and medial directions ($p \leq 0.05$, $d \geq 0.76$), as well as for internal rotators in the anterior direction ($p = 0.02$, $d = 0.96$ at JRF2) (Fig. 3). Additionally, the flexors and external rotators had higher medial forces at JRF1 ($p \leq 0.05$, $d \geq 0.52$). For individual hip muscles, the DDH group had higher forces (resultant and each component) from gluteus medius throughout stance ($p \leq 0.04$, $d \geq 0.77$; Fig. 4), and tensor fasciae latae at JRF2 ($p < 0.01$, $d \geq 1.32$).

Finally, hip JRFs were different between the DDH and Healthy groups (Fig. 3). The DDH group had significantly higher medial hip JRFs at JRF1 ($p = 0.03$, $d = 0.82$), and significantly higher resultant and superior JRFs at JRF2 ($p \leq 0.05$, $d \geq 0.76$).

3.4. Angles and moments

During late stance (at JRF2), DDH subjects had a slightly adducted hip, instead of slightly abducted for Healthy (1.2° ± 2.8° vs. −1.4° ± 2.6°, $p = 0.01$, $d = 0.95$). Also, the pelvis obliquity was towards the ipsilateral side for DDH subjects, rather than towards contralateral for Healthy (1.2° ± 2.2° vs. −1.1° ± 1.8°, $p < 0.01$, $d = 1.15$). Other hip and pelvis angles, and hip moments were not different between groups.

4. Discussion

The objective of this study was to quantify how hip muscle MALs, LoAs, and their contributions to hip JRFs during gait are altered in patients with untreated DDH compared to healthy controls. Patients with DDH demonstrated differences in both muscle anatomy (MAL, LoA) and joint mechanics (muscle force, JRF). The differences were most substantial for the hip abductor muscles, where smaller MALs corresponded to higher forces and contributions to JRFs especially in the medial direction, which supported our hypothesis. Furthermore, the inter-group differences for hip flexors and rotators exhibited how DDH alters their multi-planar functions, which suggested these muscles also contribute to atypical joint loading.

A prominent effect of the DDH bony anatomy was the shortening of dynamic MALs for the hip abductors. The abductor MALs in patients with DDH were smaller than healthy controls throughout the gait cycle, which suggest that static image-based measurements of gluteus medius MALs hold true during dynamic motions (Liu et al., 2012). The primary cause of the shortened MALs was the significantly more lateral HJC locations in untreated DDH compared to healthy hips. Shorter MALs indicate a mechanical disadvantage for the abductors, which must produce higher forces to generate the joint moment needed for hip stabilization during stance (Maquet, 1999; Neumann, 2010), thereby elevating hip JRFs. Thus, to reduce hip loading in DDH, it is important to correct the shortened abductor MALs, which can be accomplished by medializing the HJC (Gaffney et al., 2020).

Higher abductor forces may also be due to the frontal-plane MALs of the surrounding hip muscles. Three-dimensional hip motions are dependent on all muscles that span the joint, including secondary muscle functions such as the abducting effects of rectus femoris (Neumann, 2010). For DDH subjects, almost all hip muscles had less abducting or more adducting MALs compared to healthy (e.g. iliacus and rectus femoris; Table 3). Such changes in MALs altered the relative demands on each muscle to collectively produce the hip-stabilizing abduction moment (which did not differ between groups) during single-leg support. For example, while the iliacus and rectus femoris produced high forces to propel the hip forward (Suppl. Table 3), they also had an abnormal adducting effect that was then balanced by elevated hip abductor forces.

The rotation MALs of large hip muscles may also indirectly influence force production by adjacent smaller muscles, especially those with multi-planar functions. For example, the force from iliacus primarily contributes to hip flexion moments during gait. However, due to the shortened internal rotation MAL of iliacus, the tensor fasciae latae compensated with a higher-than-normal force to meet the net moment required for late-stance hip rotation

(Neumann, 2010). Therefore, due to the 3D muscle paths and outof-plane mechanics, relative contributions among adjacent muscles are integral to altered joint mechanics in the presence of DDH anatomy.

Hip muscle LoAs were less affected by the bony anatomy of untreated DDH compared to MALs. Patients with DDH had significantly more medial LoAs compared to healthy only for the gluteus maximus, although the LoAs of gluteus medius also trended towards a more medial orientation. We attribute these differences to the lateralized HJC and shape variability of the proximal femur where the gluteal muscles insert (Gaffney et al., 2019). The altered LoAs of gluteal muscles meant a higher percentage of their forces were directed medially. Therefore, to lower the elevated medial hip JRFs, reducing the dynamic medial LoAs of these muscles (e.g. via HJC medialization) may be important for clinical interventions of DDH.

The dynamic force-generating ability of hip muscles may also be affected by joint positions (Delp et al., 1999). For this cohort of patients with untreated DDH, there was a significant yet small (~2–3°) difference in hip adduction and pelvis obliquity during late stance. Hip adduction and opposite pelvis drop may be related to abductor muscle weakness (Hardcastle and Nade, 1985; Harris-Hayes et al., 2014), and may further influence their abduction MALs. However, it remains inconclusive whether such small kinematic differences are generalizable to the DDH population, or if they alter muscle mechanics in a clinically meaningful way.

Altered hip muscle anatomy or forces in DDH may not always propagate to JRF differences compared to healthy hips across the whole gait cycle. Our earlier modeling study of untreated DDH also found higher medially-directed JRFs, along with higher hip abductor muscle forces, in late stance of barefoot over-ground gait (Harris et al., 2017). Harris et al. speculated that abductor MALs were a cause of increased medial JRFs, which was confirmed by findings in the current study. In the current DDH cohort, increased abductor forces accompanied higher resultant hip JRFs only in late stance, and medial JRFs only in early stance. The contrast of hip JRF findings may be related to the gait mechanics during treadmill versus over-ground walking (Pickle et al., 2016). Nonetheless, both studies identified simultaneous elevations in hip abductor forces and medial JRFs, indicating such mechanical traits of DDH hold true while walking on flat surfaces.

Several limitations of this study must be considered. First, while we improved upon the generic model geometry by using MR-based bone-muscle anatomy, personalization of the muscle paths was limited to the static position within the MR images. Thus, inherent uncertainty exists in the model-estimated muscle paths through dynamic motions. Second, the models assumed the hip to be a rotation-only ball and socket joint. Hips with DDH may have increased instability (Wyles et al., 2017), which could induce subtle translations that change dynamic MALs and LoAs. Since hips with untreated DDH primarily lack lateral femoral coverage (Nepple et al., 2017), such instability would be most evident in the lateral direction, which would further reduce the abductor MALs. Third, we adopted and generically scaled muscle architecture parameters (e.g. fiber lengths) in our models, given that subject-specific data were unavailable. The altered muscle paths in presence of

untreated DDH anatomy could potentially lead to architectural changes, which would further affect muscle force generation and contributions to joint loading. Likewise, the efficacy of treatments for DDH may also depend on their influence on hip muscle architecture. However, our findings suggest that hip muscle MALs can already be significantly altered by DDH anatomy even in the absence of architectural adaptation. Fourth, our study was limited to gait, which is primarily a sagittal motion. It is possible that the dynamic muscle MALs, LoAs and forces in frontal and transverse planes, which were different in hips with DDH, would be further altered during multi-planar tasks such as squatting and pivoting. Lastly, while all of our DDH cohort had radiographically confirmed dysplasia, there was some heterogeneity in the severity of their bony deformities. Future research is needed to specify whether the mechanical roles of muscle MALs and LoAs change with DDH severity.

In conclusion, hip muscle MALs and contributions to JRFs were significantly altered by the abnormal bony anatomy of untreated DDH, while muscle LoAs were affected to a lesser extent. Patients with DDH demonstrated shorter hip abductor MALs than healthy controls, which corresponded to higher abductor forces. Such elevated forces are likely required to stabilize the hip in the presence of abnormal bony anatomy. Out-of-plane muscle MALs and medio-lateral LoAs also contributed to joint loading primarily in the medial direction. Thus, to better understand the mechanisms of joint degeneration and improve the efficacy of treatments for DDH, future research and interventions should collectively consider the dynamic anatomy-force relationships of the whole hip musculature and their multi-planar functions.

Supplementary Material

Refer to Web version on PubMed Central for supplementary material.

Acknowledgments

This project was supported by the National Institutes of Health K01 AR072072, P30 AR074992 and the Lottie Caroline Charitable Trust. The research content herein is solely the responsibility of the authors and does not necessarily represent the official views of the National Institutes of Health. The authors thank Molly C. Shepherd for assistance with MR image data processing.

References

Anderson FC, Pandy MG, 2001 Static and dynamic optimization solutions for gait are practically equivalent. J. Biomech 34, 153–161. [PubMed: 11165278]

Arnold AS, Salinas S, Asakawa DJ, Delp SL, 2000 Accuracy of muscle moment arms estimated from MRI-based musculoskeletal models of the lower extremity. Comput. Aided Surg 5, 108–119. [PubMed: 10862133]

Blemker SS, Delp SL, 2005 Three-dimensional representation of complex muscle architectures and geometries. Ann. Biomed. Eng 33, 661–673. [PubMed: 15981866]

Cheng R, Zhang H, Kernkamp WA, Zheng J, Dai K, Yao Y, Wang L, Tsai TY, 2019 Relations between the Crowe classification and the 3D femoral head displacement in patients with developmental dysplasia of the hip. BMC Musculoskelet. Disord 20, 530. [PubMed: 31711458]

Cohen J, 1988 Statistical Power Analysis for the Behavioral Sciences. Lawrence Earlbaum Associates, Hillsdale, NJ.

Correa TA, Crossley KM, Kim HJ, Pandy MG, 2010 Contributions of individual muscles to hip joint contact force in normal walking. J. Biomech 43, 1618–1622. [PubMed: 20176362]

De Luca CJ, Gilmore LD, Kuznetsov M, Roy SH, 2010 Filtering the surface EMG signal: Movement artifact and baseline noise contamination. J. Biomech 43, 1573–1579. [PubMed: 20206934]

Delp SL, Anderson FC, Arnold AS, Loan P, Habib A, John CT, Guendelman E, Thelen DG, 2007 OpenSim: open-source software to create and analyze dynamic simulations of movement. IEEE Trans. Biomed. Eng 54, 1940–1950. [PubMed: 18018689]

Delp SL, Hess WE, Hungerford DS, Jones LC, 1999 Variation of rotation moment arms with hip flexion. J. Biomech 32, 493–501. [PubMed: 10327003]

Faul F, Erdfelder E, Lang AG, Buchner A, 2007 G*Power 3: a flexible statistical power analysis program for the social, behavioral, and biomedical sciences. Behav. Res. Methods 39, 175–191. [PubMed: 17695343]

Gaffney BMM, Clohisy JC, Van Dillen LR, Harris MD, 2020 The association between periacetabular osteotomy reorientation and hip joint reaction forces in two subgroups of acetabular dysplasia. J. Biomech 98, 109464. [PubMed: 31708245]

Gaffney BMM, Hillen TJ, Nepple JJ, Clohisy JC, Harris MD, 2019 Statistical shape modeling of femur shape variability in female patients with hip dysplasia. J. Orthop. Res 37, 665–673. [PubMed: 30656719]

Groh MM, Herrera J, 2009 A comprehensive review of hip labral tears. Curr. Rev. Musculoskelet. Med 2, 105–117. [PubMed: 19468871]

Handsfield GG, Meyer CH, Hart JM, Abel MF, Blemker SS, 2014 Relationships of 35 lower limb muscles to height and body mass quantified using MRI. J. Biomech 47, 631–638. [PubMed: 24368144]

Hardcastle P, Nade S, 1985 The significance of the Trendelenburg test. J. Bone Joint Surg. Br 67, 741–746. [PubMed: 4055873]

Harris MD, MacWilliams BA, Bo Foreman K, Peters CL, Weiss JA, Anderson AE, 2017 Higher medially-directed joint reaction forces are a characteristic of dysplastic hips: A comparative study using subject-specific musculoskeletal models. J. Biomech 54, 80–87. [PubMed: 28233552]

Harris-Hayes M, Mueller MJ, Sahrmann SA, Bloom NJ, Steger-May K, Clohisy JC, Salsich GB, 2014 Persons with chronic hip joint pain exhibit reduced hip muscle strength. J. Orthop. Sports Phys. Ther 44, 890–898. [PubMed: 25299750]

Hermens HJ, Freriks B, Disselhorst-Klug C, Rau G, 2000 Development of recommendations for SEMG sensors and sensor placement procedures. J. Electromyogr. Kinesiol 10, 361–374. [PubMed: 11018445]

Hicks JL, Uchida TK, Seth A, Rajagopal A, Delp SL, 2015 Is my model good enough? Best practices for verification and validation of musculoskeletal models and simulations of movement. J. Biomech. Eng 137, 020905. [PubMed: 25474098]

Lai AKM, Arnold AS, Wakeling JM, 2017 Why are antagonist muscles co-activated in my simulation? A musculoskeletal model for analysing human locomotor tasks. Ann. Biomed. Eng 45, 2762–2774. [PubMed: 28900782]

Lewis CL, Sahrmann SA, 2006 Acetabular labral tears. Phys. Ther 86, 110–121. [PubMed: 16386066]

Liu R, Wen X, Tong Z, Wang K, Wang C, 2012 Changes of gluteus medius muscle in the adult patients with unilateral developmental dysplasia of the hip. BMC Musculoskelet. Disord 13, 101. [PubMed: 22703548]

MacDonald SJ, Garbuz D, Ganz R, 1997 Clinical evaluation of the symptomatic young adult hip. Semin. Arthroplasty 8, 3–9.

Maquet P, 1999 Biomechanics of hip dysplasia. Acta Orthop. Belg 65, 302–314. [PubMed: 10546353]

Moisio KC, Sumner DR, Shott S, Hurwitz DE, 2003 Normalization of joint moments during gait: a comparison of two techniques. J. Biomech 36, 599–603. [PubMed: 12600350]

Nepple JJ, Wells J, Ross JR, Bedi A, Schoenecker PL, Clohisy JC, 2017 Three patterns of acetabular deficiency are common in young adult patients with acetabular dysplasia. Clin. Orthop. Relat. Res 475, 1037–1044. [PubMed: 27830486]

Netter FH, 2014 Atlas of Human Anatomy. 6th ed W.B. Saunders, Philadelphia, PA.

Neumann DA, 2010 Kinesiology of the hip: a focus on muscular actions. J. Orthop. Sports Phys. Ther 40, 82–94. [PubMed: 20118525]

Pandy MG, 1999 Moment arm of a muscle force. Exerc. Sport Sci. Rev 27, 79–118. [PubMed: 10791015]

Pickle NT, Grabowski AM, Auyang AG, Silverman AK, 2016 The functional roles of muscles during sloped walking. J. Biomech 49, 3244–3251. [PubMed: 27553849]

Scheys L, Van Campenhout A, Spaepen A, Suetens P, Jonkers I, 2008 Personalized MR-based musculoskeletal models compared to rescaled generic models in the presence of increased femoral anteversion: effect on hip moment arm lengths. Gait Posture 28, 358–365. [PubMed: 18571416]

Shelburne KB, Decker MJ, Krong J, Torry MR, Philippon MJ, 2010 Muscle forces at the hip during squatting exercise In Proceedings of the 56th Annual Meeting of the Orthopaedic Research Society. New Orleans, LA.

Sherman MA, Seth A, Delp SL, 2013 What is a moment arm? Calculating muscle effectiveness in biomechanical models using generalized coordinates Proc. ASME Des. Eng. Tech. Conf Portland, OR.

Skalshoi O, Iversen CH, Nielsen DB, Jacobsen J, Mechlenburg I, Soballe K, Sorensen H, 2015 Walking patterns and hip contact forces in patients with hip dysplasia. Gait Posture 42, 529–533. [PubMed: 26365370]

Song K, Anderson AE, Weiss JA, Harris MD, 2019 Musculoskeletal models with generic and subject-specific geometry estimate different joint biomechanics in dysplastic hips. Comput. Methods Biomech. Biomed. Engin 22, 259–270. [PubMed: 30663342]

Steele KM, Demers MS, Schwartz MH, Delp SL, 2012 Compressive tibiofemoral force during crouch gait. Gait Posture 35, 556–560. [PubMed: 22206783]

van Arkel RJ, Modenese L, Phillips AT, Jeffers JR, 2013 Hip abduction can prevent posterior edge loading of hip replacements. J. Orthop. Res 31, 1172–1179. [PubMed: 23575923]

Wesseling M, De Groote F, Bosmans L, Bartels W, Meyer C, Desloovere K, Jonkers I, 2016a Subject-specific geometrical detail rather than cost function formulation affects hip loading calculation. Comput. Methods Biomech. Biomed. Engin 19, 1475–1488. [PubMed: 26930478]

Wesseling M, Meyer C, De Groote F, Corten K, Simon JP, Desloovere K, Jonkers I, 2016b Gait alterations can reduce the risk of edge loading. J. Orthop. Res 34, 1069–1076. [PubMed: 26632197]

Wiberg G, 1939 Studies on dysplastic acetabula and congenital subluxation of the hip joint with special reference to the complication of osteoarthritis. Acta Chir. Scand 83 (Suppl 58), 7–135.

Winter DA, 2004 Biomechanics and Motor Control of Human Movement. John Wiley & Sons, Hoboken, NJ.

Wyles CC, Heidenreich MJ, Jeng J, Larson DR, Trousdale RT, Sierra RJ, 2017 The John Charnley Award: Redefining the natural history of osteoarthritis in patients with hip dysplasia and impingement. Clin. Orthop. Relat. Res 475, 336–350. [PubMed: 27071391]

Yanagawa T, Goodwin CJ, Shelburne KB, Giphart JE, Torry MR, Pandy MG, 2008 Contributions of the individual muscles of the shoulder to glenohumeral joint stability during abduction. J. Biomech. Eng 130, 021024. [PubMed: 18412511]

Zeni JA Jr., Higginson JS, 2010 Gait parameters and stride-to-stride variability during familiarization to walking on a split-belt treadmill. Clin. Biomech. (Bristol, Avon) 25, 383–386.

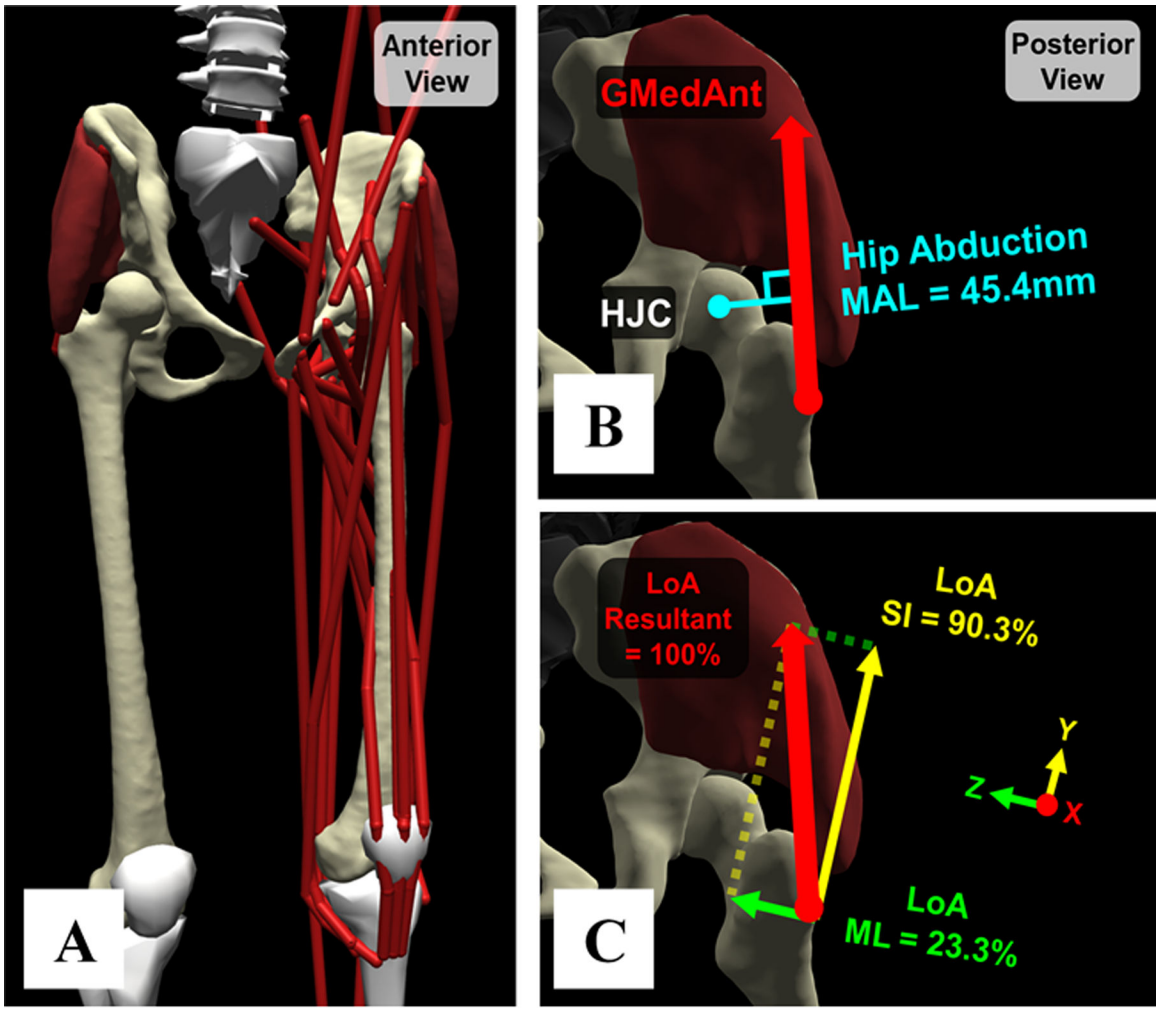

Fig. 1.

(A) Example model with subject-specific pelvis and femur geometries, HJC locations, and muscle paths. (B) Example hip muscle MAL (anterior gluteus medius, “GMedAnt”, red arrow). Hip flexion, abduction, and rotation MALs were extracted across an entire gait cycle. (C) Example hip muscle LoAs. The AP, SI, and ML components of each muscle’s LoA represent the percentage of its net force in a certain direction within the pelvis frame.

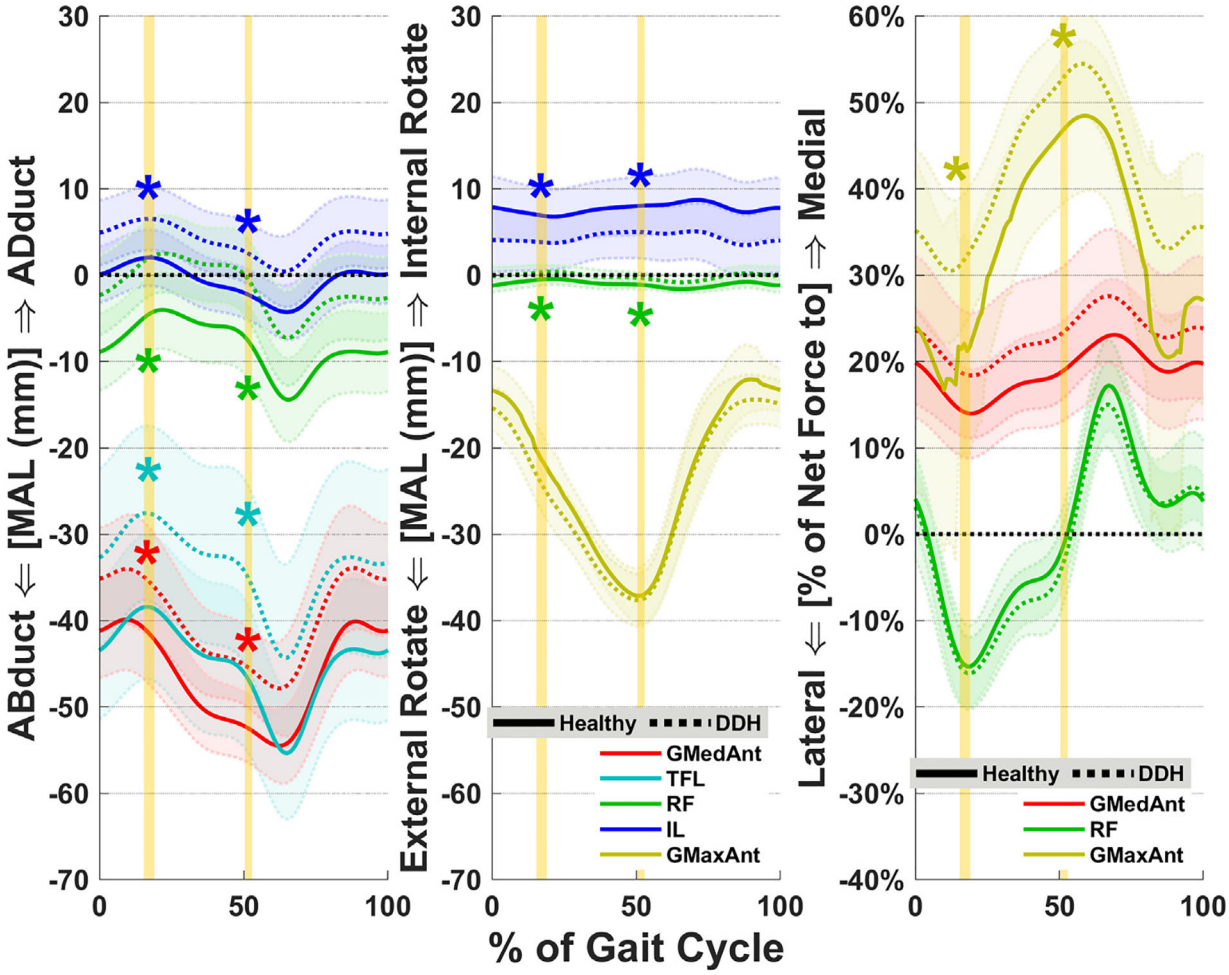

Fig. 2.

Average muscle MALs (left and center) and LoAs (right) for major hip abductors, flexors, and external rotators. Shades represent ± 1SD. Vertical highlighted areas indicate the times of JRF peaks in early stance (JRF1) and late stance (JRF2). "*" indicates statistical inter-group significance. GMedAnt, anterior gluteus medius; TFL, tensor fasciae latae; RF, rectus femoris; IL, iliacus; GMaxAnt, anterior gluteus maximus.

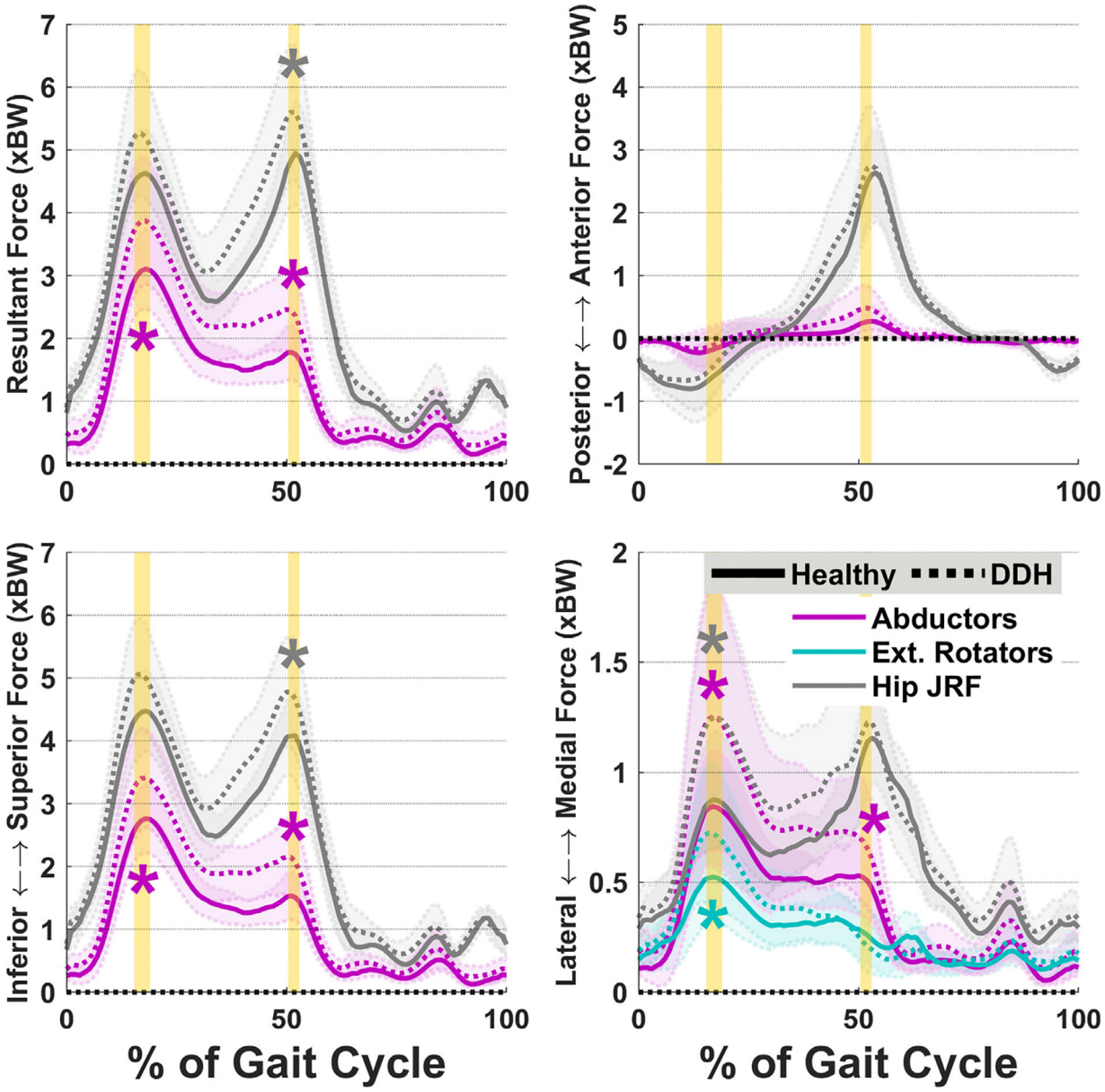

Fig. 3.

Average hip JRF components overlaid with abductor and external rotator muscle forces. Internal rotator forces (not shown) followed similar patterns to abductors. Shades represent ± 1SD. Vertical highlighted areas indicate the times of hip JRF peaks. "*" indicates statistical inter-group significance.

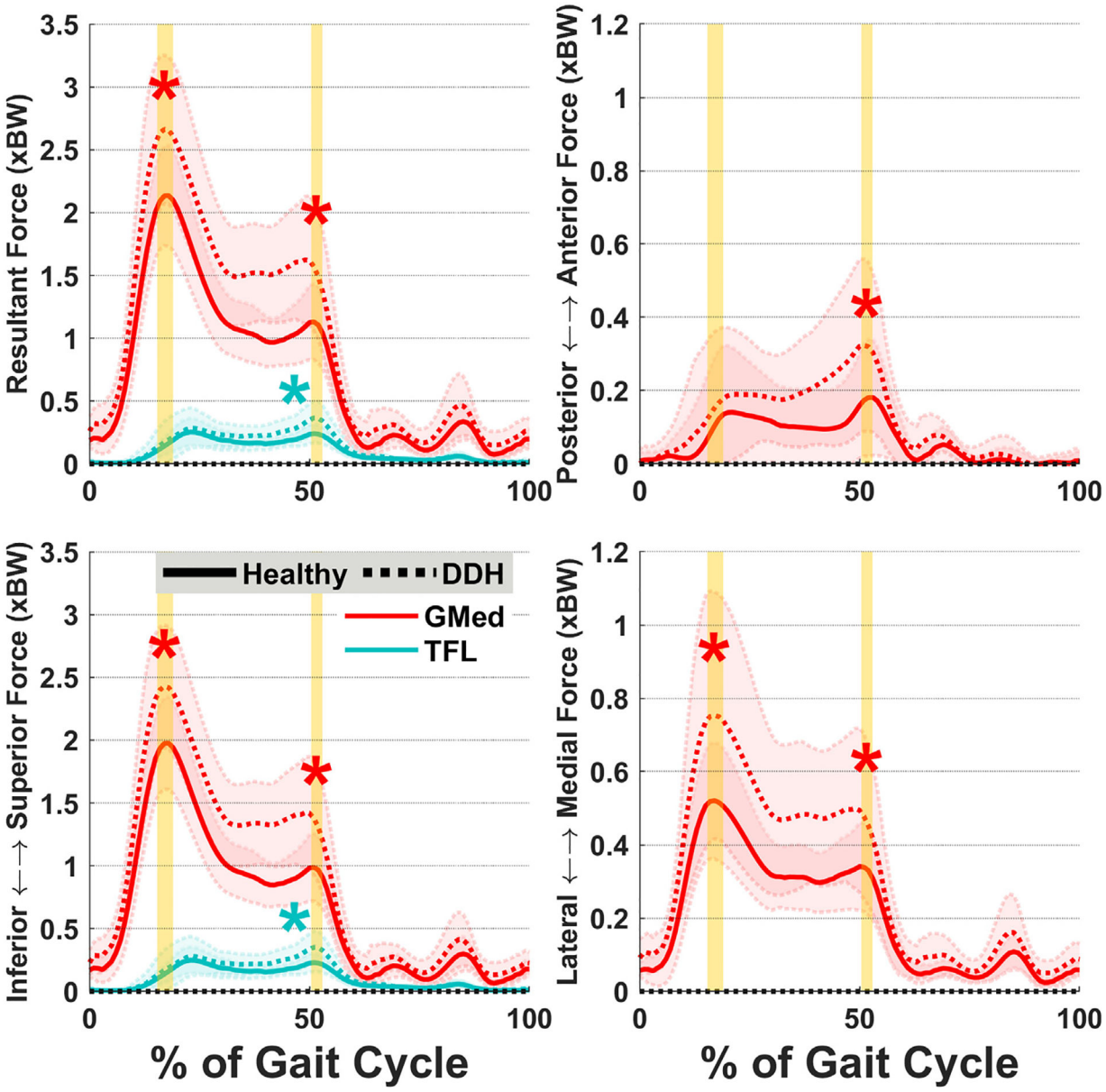

Fig. 4.

Average forces for the gluteus medius (GMed) and tensor fasciae latae (TFL) muscles. Three individual muscles had force differences between DDH and Healthy: gluteus medius, tensor fasciae latae (resultant and superior only), and gluteus minimus (similar patterns to gluteus medius). Shades represent ± 1SD. Vertical highlighted areas indicate the times of hip JRF peaks. "*" indicates statistical inter-group significance.

Table 1

Demographics, gait speed, and normalized HJC ML location (mean ± SD) for Healthy and DDH subjects.

Demographics	Healthy (N = 15)	DDH (N = 15)	*p*-value
Age (years)	24.6 ± 6.3	26.5 ± 7.9	0.62
Height (m)	1.67 ± 0.06	1.66 ± 0.07	0.85
Mass (kg)	61.9 ± 7.8	62.7 ± 9.3	0.79
BMI (kg/m^2)	22.3 ± 2.3	22.7 ± 2.4	0.64
Walking speed (m/s)	1.39 ± 0.15	1.37 ±0.15	0.59
Normalized HJC ML location (%)	77.2% ± 8.6%	88.4% ± 10.2%	< 0.01

Note: Normalized HJC ML location = ML location of HJC / ML distance between anterior superior iliac spine and mid-sagittal plane.

Table 2

Hip muscle functional group definitions.

Hip Muscle Group	Individual muscles included (alphabetic order)
Hip Flexors	adductor brevis, adductor longus, gluteus minimus (anterior), gracillis, iliacus, *pectineus, psoas major, rectus femoris, sartorius, tensor fasciae latae
Hip Extensors	adductor magnus (distal and ischial), biceps femoris long head, gluteus maximus, gluteus medius (middle and posterior), gluteus minimus (posterior), semimembranosus, semitendinosus
Hip Abductors	gluteus maximus (anterior), gluteus medius, gluteus minimus, piriformis, sartorius, tensor fasciae latae
Hip Adductors	adductor brevis, adductor longus, adductor magnus, gluteus maximus (posterior), gracillis, obturator externus, *pectineus, quadratus femoris
Hip Internal Rotators	adductor brevis, adductor longus, adductor magnus (ischial), gluteus medius (anterior), gluteus minimus (anterior), *pectineus, tensor fasciae latae
Hip External Rotators	*gemelli, gluteus maximus, gluteus medius (posterior), gluteus minimus (posterior), *obturator externus, *obturator internus, piriformis, *quadratus femoris

*Hip muscles added to the generic OpenSim musculoskeletal model. Torso muscles were also added to the model, including erector spinae, external oblique, internal oblique, and rectus abdominis (Shelburne et al., 2010).

Table 3

Dynamic MALs and LoAs (mean ± SD) for major force-generating hip muscles with significant differences (bold) between DDH and Healthy groups. LoA expressed as percentage (%) of net muscle force.

		At JRF1				At JRF2			
Hip MAL (mm)		**Healthy**	**DDH**	***p*-value**	**Cohen's *d***	**Healthy**	**DDH**	***p*-value**	**Cohen's *d***
Gluteus Medius (anterior section)	**Flexion**	6.3 ± 6.4	6.1 ± 7.6	0.94	0.03	−7.0 ± 7.2	−6.3 ± 9.1	0.82	0.08
	Adduction	**−41.6 ± 5.9**	**−35.3 ± 6.4**	**0.01**	**1.02**	**−52.6 ± 4.0**	**−45.4 ± 4.8**	**< 0.01**	**1.63**
	Rotation	24.5 ± 5.7	21.9 ± 4.8	0.19	0.49	0.1 ± 3.9	0.2 ± 6.4	0.51	0.03
Rectus Femoris	**Flexion**	40.6 ± 5.7	40.6 ± 4.8	1.00	0.00	29.4 ± 2.1	29.9 ± 2.5	0.58	0.20
	Adduction	**−4.4 ± 4.4**	**1.9 ± 4.6**	**< 0.01**	**1.41**	**−7.9 ± 4.5**	**−0.4 ± 4.9**	**< 0.01**	**1.60**
	Rotation	**−0.5 ± 0.7**	**0.3 ± 0.9**	**0.02**	**0.95**	**−1.2 ± 0.5**	**−0.3 ± 0.7**	**< 0.01**	**1.41**
Iliacus	**Flexion**	34.0 ± 3.2	35.2 ± 2.6	0.27	0.41	31.6 ±3.5	31.3 ± 3.1	0.80	0.09
	Adduction	**2.0 ± 3.3**	**6.5 ± 3.6**	**< 0.01**	**1.30**	**−2.4 ± 3.0**	**2.6 ± 3.7**	**< 0.01**	**1.46**
	Rotation	**6.9 ± 3.1**	**3.8 ± 3.3**	**0.01**	**0.95**	**8.0 ± 3.4**	**5.0 ± 3.1**	**0.02**	**0.93**
Tensor Fasciae Latae	**Flexion**	54.1 ± 10.2	57.3 ± 6.8	0.32	0.37	27.0 ± 9.4	31.9 ± 9.4	0.16	0.52
	Adduction	**−38.4 ± 8.4**	**−27.5 ± 10.1**	**< 0.01**	**1.19**	**−47.1 ± 8.6**	**−34.9 ± 10.5**	**< 0.01**	**1.28**
	Rotation	19.8 ± 4.8	21.0 ± 5.9	0.54	0.23	−0.9 ± 3.6	2.0 ± 4.9	0.07	0.68
Muscle LoA (%)		**Healthy**	**DDH**	***p*-value**	**Cohen's *d***	**Healthy**	**DDH**	***p*-value**	**Cohen's *d***
Gluteus Maximus (anterior section)	**(+) AP (−)**	−51.5 ± 15.7	−41.7 ± 10.5	0.09	0.73	−37.5 ± 13.5	−29.8 ± 8.0	0.17	0.70
	(+) SI (−)	80.4 ± 10.1	84.2 ± 4.6	0.57	0.49	78.1 ± 6.1	78.8 ± 4.8	0.72	0.13
	(+) ML (−)	**22.1 ± 12.0**	**31.5 ± 7.9**	**0.02**	0.92	**47.1 ± 8.6**	**52.8 ± 6.2**	**0.05**	**0.75**

Note: Positive values indicate hip flexion, adduction, or internal rotation MALs.